Atmos. Meas. Tech. Discuss., https://doi.org/10.5194/amt-2018-271
Manuscript under review for journal Atmos. Meas. Tech.
Discussion started: 14 November 2018

Atmospheric Measurement Techniques Discussions

Processing and quality control of FY-3C/GNOS data used in numerical weather prediction applications

Mi Liao[1], **Sean Healy**[2], Peng Zhang[1]

[1] National Satellite Meteorological Center, Beijing, China

[2] European Centre for Medium-Range Weather Forecasts, Reading, UK

Correspondence to:

Sean Healy (sean.healy@ecmwf.int), Peng Zhang (zhangp@cma.gov.cn)

Abstract

The Chinese radio occultation sounder GNOS (Global Navigation Occultation Sounder) is on the FY-3C satellite, which was launched on September 23, 2013. Currently, GNOS data is transmitted via the Global Telecommunications System (GTS) providing 450 – 500 profiles per day for numerical weather prediction applications. This paper describes the processing for the GNOS profiles with large biases, related to L2 signal degradation. A new extrapolation procedure in bending angle space corrects the L2 bending angles, using a thin ionosphere model, and the fitting relationship between L1 and L2. We apply the approach to improve the L2 extrapolation of GNOS. The new method can effectively eliminate about 90% of the large departures. In addition to the procedure for the L2 degradation, this paper also describes our quality control (QC) for FY-3C/GNOS. A noise estimate for the new L2 extrapolation can be used as a QC parameter to evaluate the performance of the extrapolation. Mean phase delays of L1 and L2 in the tangent height interval of 60 to 80 km are analysed and applied in the QC as well. A statistical comparison between GNOS and ECMWF (European Centre for Medium-Range Weather Forecasts) forecast data demonstrates that GNOS performs almost as well as GRAS, especially in the core region from around 10 to 35 km. The GNOS data with the new L2 extrapolation is suitable for assimilation into numerical weather prediction systems.

Atmos. Meas. Tech. Discuss., https://doi.org/10.5194/amt-2018-271
Manuscript under review for journal Atmos. Meas. Tech.
Discussion started: 14 November 2018

Atmospheric Measurement Techniques Discussions

1 Introduction

GNOS is the first Radio Occultation (RO) sounder on the Fengyun series of Chinese polar orbiting meteorological satellites. It is also the first multi-GNSS (Global Navigation Satellite System) RO receiver in orbit that can perform RO measurements from both GPS (Global Positioning System) and Chinese BDS (BeiDou Positioning System) signals. GNOS is manufactured by National Space Science Center (NSSC) of Chinese Academy Science (CAS), and is operated by the National Satellite Meteorological Center (NSMC) of the China Meteorological Administration (CMA). GNOS is also mounted on FY-3D (which was launched on November 2017) and it will be on all the subsequent Chinese Fengyun satellites. The FY-3 series is expected to provide GNOS RO measurements continuously at least until 2030 (Yang et al., 2012), so this is a potentially important source of data for numerical weather prediction (NWP) and climate reanalysis applications.

As a multi-GNSS receiver, GNOS has the ability of tracking up to eight GPS satellites and four BDS satellites for precise orbit determination (POD). In addition, it has velocity and anti-velocity antennas for simultaneously tracking at most six and four occultations from GPS and BDS, respectively. Because of the presence of two antennas in opposite directions, both the rising and setting occultations can be retrieved. More instrumental details are given in the Table 1, and in Bai et al. (2014). Currently, FY-3C GNOS GPS measurements can produce about 500 GPS-RO profiles per day for operational use in NWP systems, while GNOS from BDS signals are not yet operational, and produce only about 200 profiles because of fewer reference satellites.

As with the pre-existing GPS-RO sounders, such as the GPS/Met (Global Positioning System/Meteorology) experiment (Ware et al., 1996), the COSMIC (Constellation Observing System for Meteorology, Ionosphere, and Climate; Anthes et al., 2008), and the European Metop/GRAS (GNSS Receiver for Atmospheric Sounding) mission (Von Engeln et al., 2009), the raw observations from GNOS consist of phase and signal to noise ratio (SNR) measurements. In addition, auxiliary information provided by the International GNSS Service (IGS), such as the GPS

Atmos. Meas. Tech. Discuss., https://doi.org/10.5194/amt-2018-271
Manuscript under review for journal Atmos. Meas. Tech.
Discussion started: 14 November 2018

precise orbits, clock files, Earth orientation parameters, and the coordinates and measurements of the ground stations, are also needed. The IGS ultra rapid orbit products, with an approximate accuracy of 10 cm in orbit, are chosen for near-real-time operational use. The Low Earth Orbit (LEO) precise orbit determination (POD) can be estimated by integrating the equations of celestial motion (Beutler, 2005) using the Bernese software Version 5.0 (Dach et al., 2007). The single difference technique is applied to obtain the excess phase as a function of time in an Earth-centred inertial reference frame. The Radio Occultation Processing Package (ROPP) software (Version 6.0), developed by the EUMETSAT ROM SAF (Radio Occultation Meteorology Satellite Application Facility), is used to determine different kinds of atmospheric parameters (Culverwell et al., 2015). One-dimensional variational (1-D-Var) analysis, using background information from a T639L60 global forecast model, is used to retrieve temperature and humidity profiles. The T639L60 is a global medium-range weather forecast system of China, which became operational at CMA in 2009. However, since early 2017, some changes have been implemented in the operational stream. We obtain the auxiliary files through an ftp server in near real time provided by EUMETSAT GSN service, improving the timeliness to within three hours. In addition, the POD software was replaced by the PANDA (Positioning And Navigation Data Analyst), which is developed originally by the Wuhan university of China (Shi et al., 2008).

In the original operational stream, GPS-RO refractivity departure statistics were used in a preliminary check of data quality. Poor quality data was filtered out with Quality Control (QC) based on the following rules. A profile is rejected if a fractional refractivity greater than 0.1 occurs at more than 20 % levels in the profile. In addition, the outliers on a specific level are then excluded if they exceed the three sigma from a statistical point of view. This QC excluded nearly 15% GNOS profiles. We found that most of the rejected profiles had large biases of up to 200%, in the vertical interval between 5-30 km, peaking at around 20km, when compared to model data (Figure 1). These biases are not seen with other RO missions. It is known that GPS signal SNR

Atmos. Meas. Tech. Discuss., https://doi.org/10.5194/amt-2018-271
Manuscript under review for journal Atmos. Meas. Tech.
Discussion started: 14 November 2018

falls with decreasing altitudes, and especially for the L2 frequency. Therefore, in some cases the linear combination (LC) of L1 and L2 bending angles can produce erroneous results. We found that the degradation of the GNOS L2 had a large impact on the retrieval quality when the measurements were processed with ROPP. Therefore, in this work we developed and tested a new L2 bending angle extrapolation method for GNOS data, and implemented it in ROPP. As a result of this work, the GNOS data is now assimilated in operational NWP systems at, for example, the European Centre for Medium-Range Weather Forecasts (ECMWF), Deutscher Wetterdienst (DWD) and the Met Office.

In this paper, we will describe the new processing of GNOS data that reduces the large stratospheric biases in bending angle and refractivity, and present a quality control scheme for FY3C/GNOS. These results will be useful for understanding the statistical error characteristics and quality control of the GNOS data, and more generally the extrapolation approach may useful for other missions where one signal is lost early.

2 Large biases in the original GNOS processing

The ROPP software (Culverwell et al., 2015) is used to retrieve atmospheric parameters, such as bending angle, refractivity, dry temperature, temperature and humidity, from GNOS excess phase measurements. In the preliminary assessments for the FY-3C/GNOS GPS RO against NWP with the original processing system, it was found that the most obvious and prominent quality issue was the large departure biases, in the vertical range of 5-30 km, peaking at around 20km (Figure 1). The percentage of profiles effected was about 13~15%. This bias problem is not seen with other RO missions, and it was found to be related to GPS L2 signal tracking problems and the subsequent extrapolation of L2.

It was found that most of the bad cases are rising occultations, which is easy to understand. To improve the tracking in the lower troposphere and the quality of rising occultations, open loop tracking is implemented for GNOS GPS L1 signal, but not for

Atmos. Meas. Tech. Discuss., https://doi.org/10.5194/amt-2018-271
Manuscript under review for journal Atmos. Meas. Tech.
Discussion started: 14 November 2018

L2 (Ao et al., 2009). In general, the SNR falls under the complicated atmospheric conditions in troposphere because of atmospheric defocusing. The GPS L2 signal is modulated by a pseudo-random precision ranging code (P code) for the purpose of anti-spoofing. Although GPS L2 can be demodulated using the semi-codeless method, it will be at the expense of SNR and precision (Kursinski et al., 1997). Therefore, the performance of L2 signal tracking is not as good as L1, especially for the rising occultations. Figure 2 shows the lowest Straight Line Tangent Altitude (SLTA) percentages of L1 and L2 signals, for both the rising and the setting occultations. It shows that the lowest tracking height of L1 C/A of both the rising or setting measurements are reasonable, with more than 98.5% profiles with a below zero SLTA. However, for the L2P, only 70% of the rising measurements reach below 20km. There are 24.8% of rising profiles stopping in the range of 20 ~70km, and 5.2% stopping above 70km, meaning effectively they contain no valid measurements. In contrast, 89.9% of setting occultations can get below 20km, which is better than the rising, but about 10% stop above that height. Those profiles that have bad L2 signal observations significantly affect the retrievals when using ROPP software to process the GNOS data.Figure 3 shows an example of GNOS performance in terms of excess phase, SNR, and bending angle for two bad cases where the L2 stops early. In these two cases, there are no valid L2 excess phase observations below 25km or 30km SLTA, respectively. However, there are L2 bending angles, extending to the near surface because of extrapolation within ROPP (ROM SAF, 2016). Although this ROPP extrapolation approach may be reasonable for other missions where L2 penetrates deeper, it does not appear to be valid for GNOS.

Figure 4 is the same as Figure 3 but for two good cases where the L2 measurements get to 20km SLTA. Compared with the bad cases, the good cases show deeper penetration for L2. Thus, the retrieved bending angles of L1, L2 and LC are overlapping, and show good consistency even at the lower part of the profiles.

Atmos. Meas. Tech. Discuss., https://doi.org/10.5194/amt-2018-271
Manuscript under review for journal Atmos. Meas. Tech.
Discussion started: 14 November 2018

3 New L2 extrapolation

As mentioned in the Section 2, some sort of extrapolation of the observed L2 signal is required before it can be combined with the L1 signal, in order to remove the ionospheric contribution to the bending. However, the current L2 extrapolation implemented in ROPP leads to obvious errors when processing GNOS RO data. Therefore, an alternative L2 extrapolation method has been implemented in the ROPP to solve the GNOS problem. The new approach is based on (unpublished) work by Culverwell and Healy (2015), who modelled the bending angles produced by a Chapman layer model ionosphere and other profiles, and established some basic theory for the relationship between fitting L1 and L2. The method adopted here is based on a "thin" ionospheric shell model, where the ionosphere approaches a Delta function, at a specified height (See section 3.1, Culverwell and Healy, 2015). Alternative approaches are described by Zeng. et al., (2016).

For a vertically localized region of refractivity, sited well above tangent points of interest, the ionospheric contribution to the bending angle, α, at frequency f can be simply expressed by (Eq. 2.6, Culverwell and Healy, 2015):

$$\alpha(a) = 2a\frac{k_4}{f^2}\int_a^\infty \frac{x n_e(x)}{(x^2-a^2)^{\frac{3}{2}}}dx \qquad (3.1)$$

where $x = nr$, is product of the refractive index, n, and radius value r, a is the impact parameter, $k_4 = \frac{e^2}{8\pi^2 m_e \varepsilon_0} = 40.3 m^3 s^{-2}$, and n_e is the electron number density. Commonly, the electron number density can be expressed in terms of the vertically integrated total electron content, TEC, which is defined as $TEC = \int n_e dr$. The equation above can be simplified by assuming a very narrow ionospheric shell and written as (Eq. 3.2, Culverwell and Healy, 2015):

$$\alpha(a) = 2a\frac{k_4}{f^2} TEC \frac{r_0}{(r_0{}^2-a^2)^{\frac{3}{2}}} \qquad (for\ a < r_0) \qquad (3.2)$$

r_0 is height of the peak electron density, which is assumed to be 300 km above the surface in this work.

Atmos. Meas. Tech. Discuss., https://doi.org/10.5194/amt-2018-271
Manuscript under review for journal Atmos. Meas. Tech.
Discussion started: 14 November 2018

Atmospheric Measurement Techniques Discussions

The GPS L1 and L2 frequency bending angle difference is expressed as:

$$\alpha_2(a) - \alpha_1(a) = 2ak_4TEC\left(\frac{1}{f_2^2} - \frac{1}{f_1^2}\right)\frac{r_0}{(r_0{}^2 - a^2)^{\frac{3}{2}}} \qquad (3.3)$$

If we define $x_{so} = 2ak_4TEC\left(\frac{1}{f_2^2} - \frac{1}{f_1^2}\right)$, then,

$$\alpha_2(a) = \alpha_1(a) + x_{so}\frac{r_0}{(r_0{}^2 - a^2)^{\frac{3}{2}}} \qquad (3.4)$$

In this work we estimate x_{so} from a least-square fit based on observed L1 and L2 bending angle differences produced with geometrical optics, over a 20 km vertical above the lowest valid L2 bending angle value. The maximum height of the vertical interval is limited to be 70 km.

Two bad profiles, where the L2 signal stops above 20 km SLTA, have been chosen for demonstrating the extrapolation method. Their detailed information is listed in Table 2. Because the ionospheric effect becomes smaller in relative terms with the decreasing height, the magnitude of the relative L2-L1 bending angle differences gets smaller with height. Seen from the direct comparisons between the new and the old extrapolation results of case 1 (Figure 5 and 6), L2 is very different to L1 before correction. After applying the new extrapolation approach, the L2 bending angles below 20 km are consistent with both L1 and LC. It is concluded that a more reliable LC bending angle can be obtained by using the new L2 extrapolation approach than the original L2 extrapolation method implemented in ROPP.

Clearly, using the new simple ionospheric model for the L2 extrapolation performs very well for the bad profiles with large biases. It is also useful to demonstrate the new extrapolation method for normal cases. Here the normal profiles are defined as the lowest SLTA reaching below 20 km, and the mean standard deviation to the reanalysis data is within 2% from surface to 35 km. Therefore, two good profiles (Table 3) are selected to test the new extrapolation.

Generally, the new extrapolation method does not degrade the good profiles. In fact, the new method smooths some occultation points, and improves the consistency of L1 and L2, as shown in Figure 7 and 8, for example.

An alternative way to demonstrate the accuracy of the different extrapolation methods is to compare their refractivity retrievals with the forecast model data. One

Atmos. Meas. Tech. Discuss., https://doi.org/10.5194/amt-2018-271
Manuscript under review for journal Atmos. Meas. Tech.
Discussion started: 14 November 2018

day of data is used to test the new L2 extrapolation method. Figure 9 shows that the new method can effectively eliminate ~90 % of the problematic "branches" with the large percentage refractivity errors often are exceeding 100 %. In this plot, eight profiles still have a large bias after the new extrapolation, because the L2 SLTA stops above 70 km, which is out of the processing range used in the extrapolation (below 70 km). These cases can be removed by including some simple additional QC steps.

4 Quality control methods

Although the new L2 extrapolation method removes more than 90% poor quality profiles, there are still some profiles with obvious errors. Therefore, additional QC methods need to be implemented. Based on the GPS RO error sources and characteristics, many internal QC methods have proposed in the literature. For example, the COSMIC Data Analysis and Archive Center (CDAAC) define an altitude, *Z*, below which a low quality of L2 signal has been detected. The maximum difference of Ll and L2 bending angle above Z, and the ionospheric scintillation index analyzed from the amplitude of L1 signal at high altitudes are used in the QC (Kuo et al., 2004). Gorbunov (2002) proposed a QC procedure in terms of the analysis of the amplitude of the RO data transformed by the Canonical Transform (CT) or the Full Spectrum Inversion (FSI) method (Gorbunov and Lauritsen, 2004), which is useful to catch the corrupted data because of phase lock loop failures. Beyerle et al. (2004) also suggested a QC approach to reject the RO observations degraded by ionospheric disturbances based on the phase delay of L1 and L2 signals.

In light of the characteristics of GNOS RO data, we developed and tested some new internal QC methods to detect the poor quality profiles.

4.1 Noise estimate of the L1 and L2 fit

As noted earlier, as a result to L2 signal tracking problems, around 15% profiles are degraded with the old processing. After applying the new L2 extrapolation method, most of them can be effectively corrected. As seen from the Eq. 3.4, the key to the

Atmos. Meas. Tech. Discuss., https://doi.org/10.5194/amt-2018-271
Manuscript under review for journal Atmos. Meas. Tech.
Discussion started: 14 November 2018

Atmospheric Measurement Techniques Discussions

correction is how well the retrieved parameter, x_{so}, fits the difference of L1 and L2 bending angles in the 20km fitting interval. Currently, 25 km or the minimum L2 SLTA is the lower limit of the fitting interval.

We have introduced a new parameter, *noise_estimate*, to test the quality of the least-square fit in the 20 km interval. It can be expressed as:

$$noise_{\_estimate} = \frac{\sqrt{\sum(x_{so} * \frac{r_0}{(r_0{}^2 - a^2)^{\frac{3}{2}}} - \Delta\alpha(a))^2}}{n} * 10^6 \quad (4.1)$$

Where $\Delta\alpha$ is the difference of L1 and L2 bending angles, and the sum is over the 20 km fitting interval. The physical meaning of *noise_estimate* is easy to understand. It is the standard deviation of the difference between the fit and observations. If the *noise_estimate* is small, x_{so}, is fitted well, then the L2 extrapolation using the x_{so} is probably adequate.

A histogram of the *noise_estimate* values has been obtained by accumulating statistics over a seven day period (Figure 10), and we use this to determine a QC threshold value. In the operational GNOS processing, if the value of the *noise_estimate* is greater than 20 micro-radians, the profiles will be rejected. We have used one day of data to test the performance of the *noise_estimate* as a QC parameter, for detecting the large bias cases. The *noise_estimate* of the good profiles are highly focused on the values are below 20; while the *noise_estimate* of the bad profiles, with large biases, have the largest *noise_estimate* values. It demonstrates that setting the *noise_estimate* parameter threshold at 20 microradians can distinguish between many of the good and the bad GNOS cases. This parameter can be used as one factor, but other parameters are still needed to complete the QC.

4.2 Mean phase delays of L1 and L2

The *noise_estimate* QC parameter does not detect all the poor quality profiles, and we need extra quality control methods to identify them. We find that it is also necessary to monitor the performance of GNOS mean L1 and L2 phase delays in the height interval of 60 to 80 km, because this can also indicate the observational quality

Atmos. Meas. Tech. Discuss., https://doi.org/10.5194/amt-2018-271
Manuscript under review for journal Atmos. Meas. Tech.
Discussion started: 14 November 2018

of GPS RO data. However, the L1 and L2 SNR values, that are commonly used as a QC indicator, are not found to be useful for identifying the large bias cases of GNOS data.

Figure 11 and Figure 12 show the histograms of the L1 and L2 mean delay phase in rising occultations. They show that there is a clear relationship between the poor profiles and the mean phase delay of L1 and L2. Therefore, we can identify most of the bad rising occultations, when both L1 and L2 mean phase values are greater than -150 m. Unavoidably, a few of the good profiles could be wrongly detected as well and few bad ones could be missed. However, the statistical performance is reasonable, as will be demonstrated in Section 4.3.

4.3 The statistical performance of the applied QC methods

After checking a number of QC parameters, we use the following three QC tests:

(1) If the occultation is rising, and the both mean phase delays of L1 and L2 are greater than -150m, the profile will be identified as “bad”;

(2) If the value of *noise_estimate* is greater than 20 microradians, the profile will be identified as “bad”;

(3) If the lowest SLTA of L2 is greater than 50 km, the profile will be identified as “bad”.

For example, these have been tested with one day of data, as to whether they can identify the “bad” large bias cases. The percentage of the bad profiles for one day is 9.7% of the data. After applying the QC method, the ratio of the profiles identified as “bad” is 11.1%. It can be correctly identified 8.0% of the bad profiles, which means 3.1% profiles are mistakenly identified and 1.7% of the profiles are still missing (Table 4). In general, the performance of this kind of QC method can effectively identify most of the bad profiles.

Atmos. Meas. Tech. Discuss., https://doi.org/10.5194/amt-2018-271
Manuscript under review for journal Atmos. Meas. Tech.
Discussion started: 14 November 2018

5 Comparison with ECMWF forecast data

This section demonstrates the performances of the comparison between the observational GNOS bending angles and the simulated ones using ECMWF short-range forecast data. GNOS bending angle profiles are those which are carried out using the new L2 extrapolation and quality controls mentioned in section 3 and section 4, respectively. The period is from 6th July to 2nd Aug. 2018. The ECMWF data used as the background is the state-of-the-art short-range forecast data with 137 vertical levels extending from surface to 0.01 hPa. Using the 2D bending angle forward operator, ECMWF forecast data can be projected into the bending angle space at the GNOS locations.

GNOS observations are provided BUFR format for NWP applications, with the bending angles given on 247 vertical levels from the surface to 60 km. To provide a context for the comparisons, Metop-A GRAS profiles from the same period are also selected as a benchmark. Figure 13 displays the mean bias for the GNOS and GRAS bending angle profiles both separated into rising and setting occultations, showing that GNOS and GRAS are very consistent with each other above 10 km. Figure 14 shows the standard deviation of the bending angle departures for the GNOS and GRAS. Their standard deviations are about 1% between 10 – 35 km, increasing to about 12% at 50 km and more than 15% below 5 km impact height. It is clear that the GNOS standard deviations are comparable to GRAS in the 10 - 40km interval. The difference in the 20 to 25 km interval is related to the transition from wave optics to geometric optics for the GNOS. The GRAS standard deviations are worse in the troposphere but this is probably due to sampling; essentially GRAS is able to measure more difficult cases. Generally, the two datasets have similar error characteristics in terms of both the mean bias and standard deviation over most of the height interval, but especially in the GPS-RO core range between 10-35 km.

6 Conclusions

This study has focused on three main areas. Firstly, we have developed and tested a new L2 extrapolation for GNOS GPS-RO profiles. Secondly, we have

investigated QC methods for GNOS after applying the new L2 extrapolation. Thirdly, we have estimated the bending angle departure statistics by comparing GNOS and ECMWF short-range forecast data. The main results are summarized below.

We have identified and investigated the GNOS GPS-RO cases that fail quality control with large bending angle departures, after the processing with the ROPP software. These large departures can be attributed to the GPS L2 signal tracking problems for signals that stop above 20 km in terms of SLTA, and the related L2 extrapolation. The percentage of the profiles with large departure is about 13~15%. Therefore, we focused on a better L2 extrapolation for GNOS when L2 signal stops early. A new L2 extrapolation approach has been implemented in ROPP to mitigate the problem. (These modifications will be available in ROPP 9.1; see http://www.romsaf.org/ropp/) The main procedure is in bending angle space, and it is based on the (unpublished) study of Culverwell and Healy (2015). The new method can effectively remove about 90% of the large departures. The remaining poor cases are mostly due to the L2 being completely missing.

We have studied and established the quality control methods suitable for GNOS GPS-RO profiles after correcting the large departures. The new L2 extrapolation *noise_estimate* value can be taken as a QC parameter to evaluate the performance of the extrapolation. It is the standard deviation of the difference between the fit and observations above the extrapolated height. The mean phase delays of L1 and L2 in the tangent height interval of 60 to 80 km are analysed and applied in the QC as well. The lowest SLTA of L2 is also set as a threshold to identify the bad profiles. Using the parameters mentioned above, the QC method can identify 82.5% of the bad profiles with a mean bias is greater than 5%.

Finally, we have assessed the quality of the GNOS bending angles by comparing with operational ECMWF short-range forecasts. GRAS profiles from the same period are selected as a benchmark. The departure statistics for the GNOS and GRAS bending angle profiles in terms of the mean bias and standard deviations are similar at most of the heights, especially in the GPS-RO core region between 10-35 km.

The GNOS measurements processed with methods outlined in this study have been assimilated into operational NWP systems since March 6, 2018.

Acknowledgments

This work was undertaken as part of a visiting scientist study funded by the Radio Occultation Meteorology Satellite Application Facility (ROM SAF), which is a decentralised processing centre under the European Organisation for the Exploitation of Meteorological Satellites (EUMETSAT).

We have to express my appreciation to Christian Marquardt for his valuable suggestions with respect to the RO processing and QC methods. In addition, we want to thank Ian Culverwell and Chris Burrow for their discussions. Finally, we would like to thank the fund support of National Key R&D Program of China (No.*2018YFB0504900*) and Special Fund for Meteorology Research in the Public Interest (No.*201506074)*.

References

Anthes, R. A., Ector, D., Hunt, D. C., Kuo, Y.-H., Rocken, C., Schreiner, W. S., Sokolovskiy, S. V., Syndergaard, S., Wee, T.- K., Zeng, Z., Bernhardt, P. A., Dymond, K. F., Chen, Y., Liu, H., Manning, K., Randel, W. J., Trenberth, K. E., Cucurull, L., Healy, S. B., Ho, S.-P., McCormick, C., Meehan, T. K., Thompson, D. C., and Yen, N. L.: The cosmic/formosat-3 mission: Early results, B. Am. Meteorol. Soc., 89, 313–333, 2008.

Ao, C. O., Hajj, G. A., Meehan, T. K., Dong, D., Iijima, B. A., Mannucci, J. A., and Kursinski, E. R.: Rising and setting GPS occultations by use of open-loop tracking, J. Geophys. Res., 114, D04101, doi:10.1029/2008JD010483, 2009.

Bai, W. H., Sun, Y. Q., Du, Q. F., Yang, G. L., Yang, Z. D., Zhang, P., Bi, Y. M., Wang, X. Y., Cheng, C., and Han, Y.: An introduction to the FY3 GNOS instrument and mountain-top tests, Atmos. Meas. Tech., 7, 1817–1823,

doi:10.5194/amt-7-1817-2014, 2014.

Beutler, G.: Methods of Celestial Mechanics, Springer-Verlag, Berlin, Heidelberg, New York, Germany, USA, ISBN 3-211- 82364-6, 2005.

Beyerle, G., 1. Wickert., T Schmidt, and C. Reigber., Atmospheric sounding by GNSS radio occultation: An analysis of the negative refractivity bias using CHAMP observations, J Geophys.Res., 109, D01106, doi:10.102912003JD003922,2004.

Culverwell, I. D. and S. B. Healy: Simulation of L1 and L2 bending angles with a model ionosphere, ROM SAF Report 17, 2015. Available at http://www.romsaf.org/general-documents/rsr/rsr_17.pdf, 2015.

Culverwell, I. D., Lewis, H. W., Offiler, D., Marquardt, C., and Burrows, C. P.: The Radio Occultation Processing Package, ROPP, Atmos. Meas. Tech., 8, 1887-1899, https://doi.org/10.5194/amt-8-1887-2015, 2015.

Dach, R., Hugentobler, U., Fridez, P., and Meindl, M.: Bernese GPS Software Version 5.0. Astronomical Institute, University of Bern, Switzerland, 2007.

Gorbunov, M. E.: Ionospheric correction and statistical optimization of radio occultation data, Radio Sci., 37, 17-1–17-9, doi:10.1029/2000RS002370, 2002.

Gorbunov, M. E. and Lauritsen, K. B.: Analysis of wave fields by Fourier Integral Operators and their application for radio occultations, Radio Sci., 39, RS4010, doi:10.1029/2003RS002971, 2004.

Kuo, Y.-H., Wee, T.-K., Sokolovskiy, S., Rocken, C., Schreiner, W., Hunt, D., and Anthes, R. A.: Inversion and error estimation of GPS radio occultation data, J. Meteor. Soc. Japan, 82, 507–531,2004.

Kursinski, E. R., Hajj, G. A., Hardy, K. R., Schofield, J. T., and Lin- field, R.: Observing Earth's atmosphere with radio occultation measurements, J. Geophys. Res., 102, 23429–23465, 1997.

ROM SAF http://www.romsaf.org/product_documents/romsaf_atbd_ba.pdf, 2016.

Shi C, Zhao Q, Lou Y. Recent development of PANDA software in GNSS data processing[J]. Proc. SPIE, 7285:231-249, 2008.

Von Engeln, A., Healy, S., Marquardt, C., Andres, Y., and Sancho, F.: Validation of

operational GRAS radio occultation data, Geo- phys. Res. Lett., 36, L17809, doi:10.1029/2009GL039968, 2009.

Ware, R., Rocken, C., Solheim, F., Exner, M., Schreiner, W., An- thes, R., Feng, D., Herman, B., Gorbunov, M., Sokolovskiy, S., Hardy, K., Kuo, Y., Zou, X., Trenberth, K., Meehan, T., Melbourne, W., and Businger, S.: GPS sounding of the atmosphere from lower Earth orbit: preliminary results, B. Am. Meteorol. Soc., 77, 19–40, 1996.

Yang, J., Zhang, P., Lu, N.-M., Yang, Z.-D., Shi, J.-M., and Dong, C.-H.: Improvements on global meteorological observations from the current Fengyun 3 satellites and beyond, Int. J. Digital Earth, 5, 251–265, 2012.

Zeng.Z., Sokolovskiy,S., Schreiner,W., Hunt,D., Lin,J., and Kuo,Y.-H.: Ionospheric correction of GPS radio occultation data in the troposphere, Atmos. Meas. Tech., 9, 335–346, 2016.

Atmos. Meas. Tech. Discuss., https://doi.org/10.5194/amt-2018-271
Manuscript under review for journal Atmos. Meas. Tech.
Discussion started: 14 November 2018

Atmospheric Measurement Techniques Discussions

Table 1 Main instrumental parameters for FY-3C/GNOS

Parameters	FY-3C/GNOS
Orbit Height	~836 km
Orbit Type	sun synchronous
Spacecraft mass	~750kg
Instrument mass	7.5kg
Constellation	GPS L1 C/A, L2 P
	BDS B1I,B2I
Channels	GPS：14 BDS：8
Sampling	POD 1Hz
	ATM.occ. (closed loop)50Hz
	ATM.occ.(open loop) 100 Hz
	ION occ. 1Hz
Open loop	GPS L1 C/A
Clock stability	1×10－12（1secAllan）
Pseudo-range precision	≤30cm
Carrier phase precision	≤2mm
Beam width of atmosphere occultation antenna	≥±30°(azimuth)

Atmos. Meas. Tech. Discuss., https://doi.org/10.5194/amt-2018-271
Manuscript under review for journal Atmos. Meas. Tech.
Discussion started: 14 November 2018

Table 2. Details of the selected bad occultations

No.	Occ. time (yymmdd.hhmm)	Longitude (deg.)	Latitude (deg.)	Occ. direction	SLTA_L2 (km)
1	170128.0332	-99.154	25.070	rising	21.917
2	170128.0740	24.705	-4.222	rising	25.793

Table 3. Details of the good profiles

No.	Occ. time (yymmdd.hhmm)	Longitude (degree)	Latitude (degree)	Occ. direction	SLTA_L2 (km)
1	20170128.0103	149.508	-38.445	rising	4.011
2	20170128.0251	70.857	-51.463	rising	12.928

Table 4. The 2×2 table values

		Bad case (True)	
		YES	NO
Bad case (Identified by QC parameters)	YES	8.0% (hits)	3.1%(false identified)
	NO	1.7%(misses)	87.2%(correct negatives)

Atmos. Meas. Tech. Discuss., https://doi.org/10.5194/amt-2018-271
Manuscript under review for journal Atmos. Meas. Tech.
Discussion started: 14 November 2018

Atmospheric Measurement Techniques Discussions

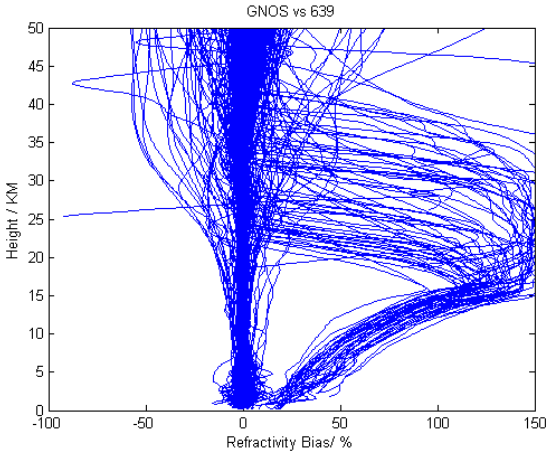

Figure 1. FY-3C/ GNOS GPS refractivity bias compared to T639 (the Chinese forecast model data), on 28th Jan.2017 with 489 samples.

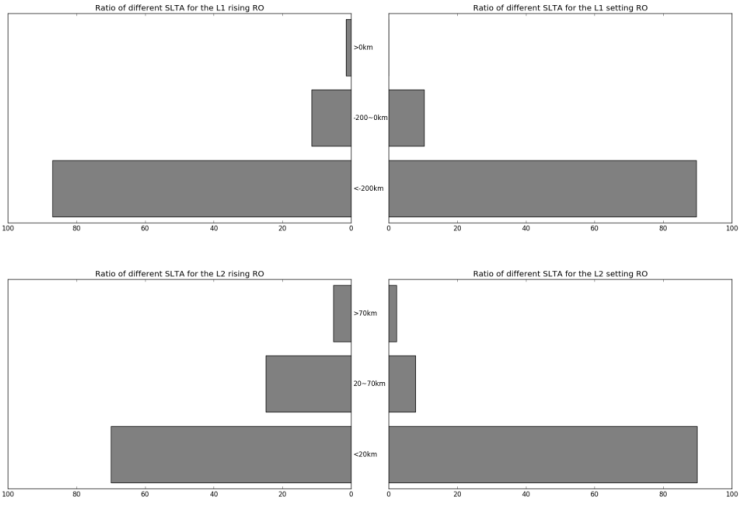

Figure 2. Ratio of different SLTA of the L1 C/A and L2 P for the rising and setting occultations, statistics result is from 28th Jan to 2nd Feb. 2017.

Atmos. Meas. Tech. Discuss., https://doi.org/10.5194/amt-2018-271
Manuscript under review for journal Atmos. Meas. Tech.
Discussion started: 14 November 2018

Atmospheric Measurement Techniques Discussions

(a)

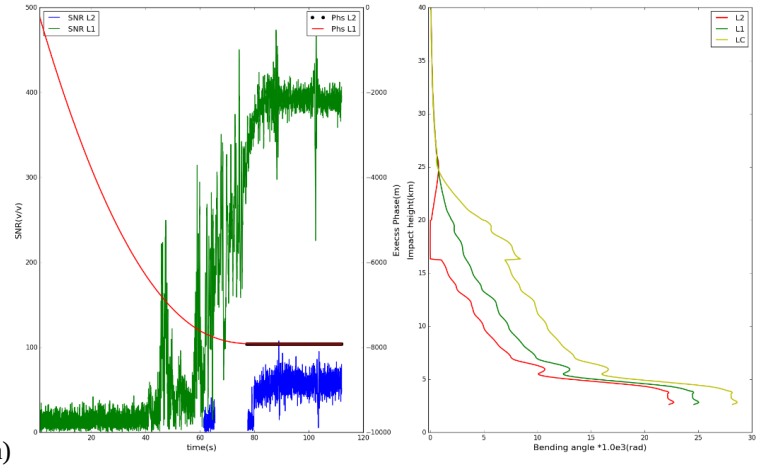

(b)

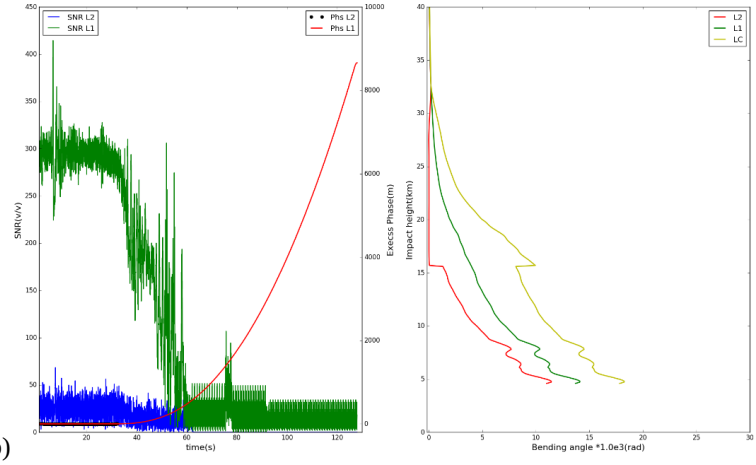

Figure 3. Two bad cases (a) A rising profile (FY3C_GNOSX_GBAL_L1_20170128_0332_AEG15_MS.NC), (b) a setting profile (FY3C_GNOSX_GBAL_L1_20170128_0850_AEG18_MS.NC). Example L1 (red) and L2 (black) SNR and excess phase measured data. The resulting L1 bending angle (green), L2 bending angle (red), and LC bending angle (yellow) profiles as a function of impact parameter computed using ropp_pp routines.

Atmos. Meas. Tech. Discuss., https://doi.org/10.5194/amt-2018-271
Manuscript under review for journal Atmos. Meas. Tech.
Discussion started: 14 November 2018

Atmospheric Measurement Techniques Discussions

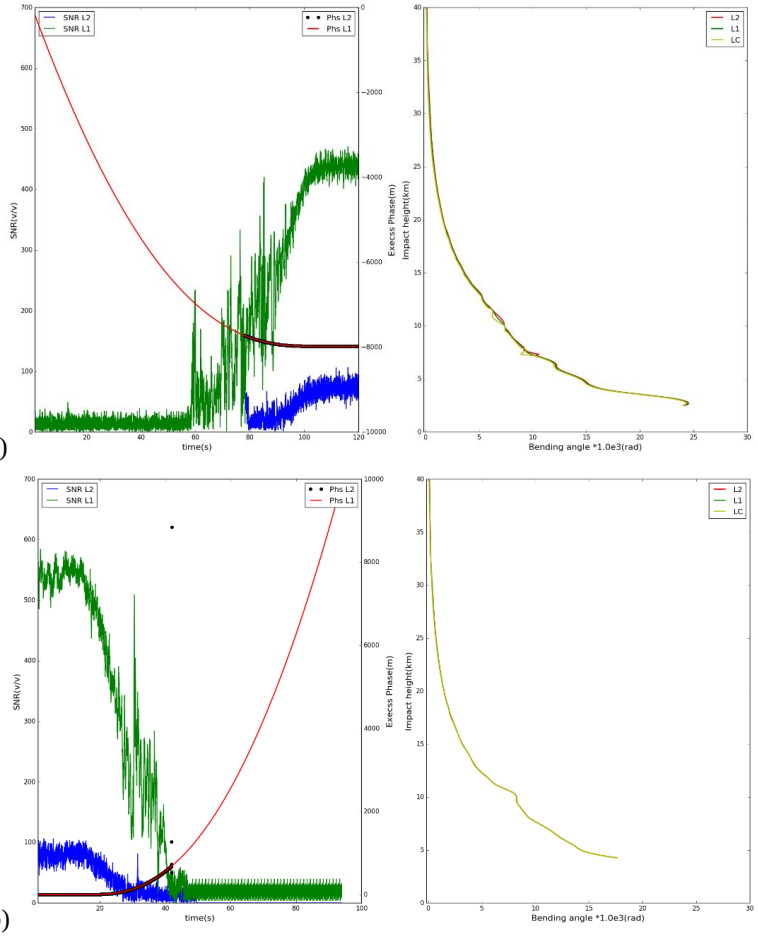

(a)

(b)

Figure 4. Two good cases (a) A rising profile (FY3C_GNOSX_GBAL_L1_20170128_1138_AEG27_MS.NC), (b) a setting profile (FY3C_GNOSX_GBAL_L1_20170128_1648_AEG31_MS.NC). Example L1 (red) and L2 (black) SNR and excess phase measured data. The resulting L1 bending angle (green), L2 bending angle (red), and LC bending angle (yellow) profiles as a function of impact parameter computed using ROPP routines.

Atmos. Meas. Tech. Discuss., https://doi.org/10.5194/amt-2018-271
Manuscript under review for journal Atmos. Meas. Tech.
Discussion started: 14 November 2018

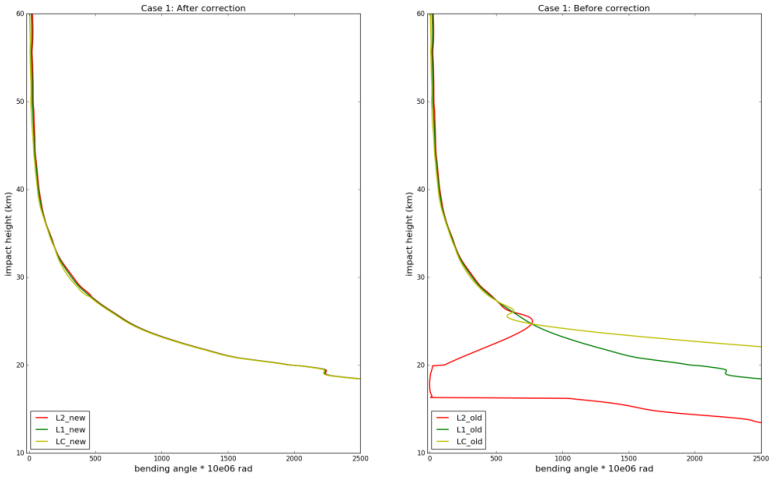

Figure 5. Case1: the bending angle of L2 (red), L1 (green) and LC (yellow) before (right) and after (left) correction.

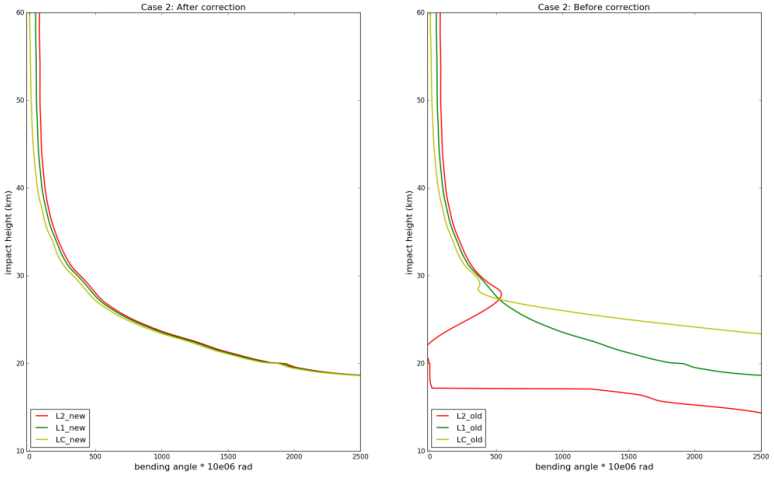

Figure 6. The same as Figure 5 but for Case 2.

Atmos. Meas. Tech. Discuss., https://doi.org/10.5194/amt-2018-271
Manuscript under review for journal Atmos. Meas. Tech.
Discussion started: 14 November 2018

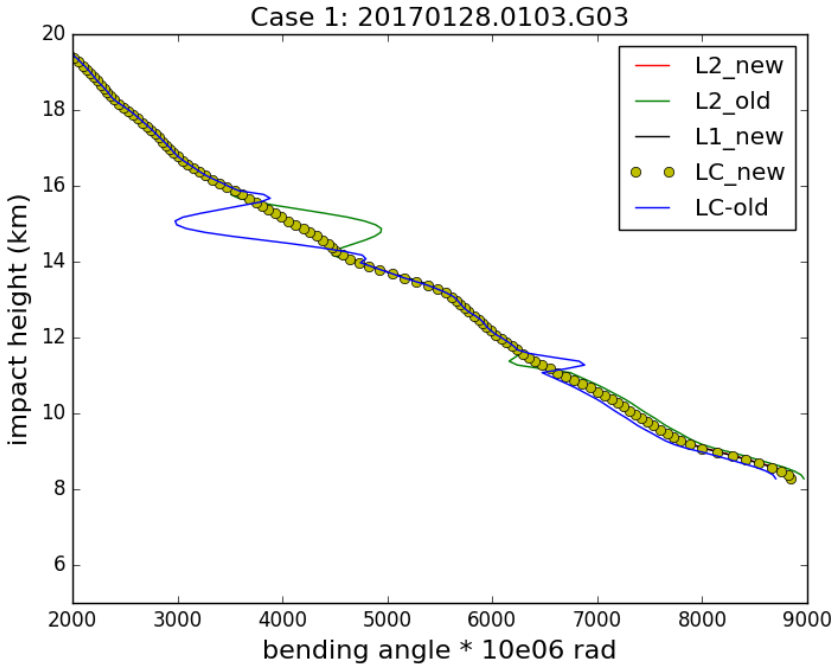

Figure 7. Good Case 1: the bending angle of L2, L1 and LC before and after correction.

Atmos. Meas. Tech. Discuss., https://doi.org/10.5194/amt-2018-271
Manuscript under review for journal Atmos. Meas. Tech.
Discussion started: 14 November 2018

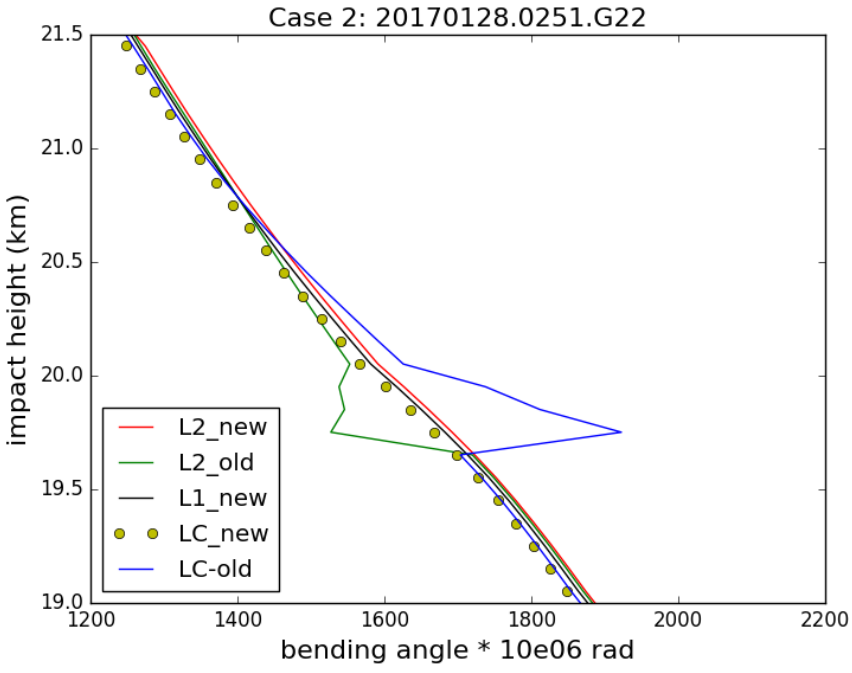

Figure 8. Good Case2: the bending angle of L2, L1 and LC before and after correction.

Atmos. Meas. Tech. Discuss., https://doi.org/10.5194/amt-2018-271
Manuscript under review for journal Atmos. Meas. Tech.
Discussion started: 14 November 2018

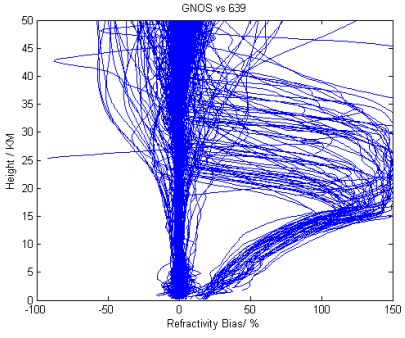

Figure 9. FY-3C/ GNOS GPS refractivity bias compared to T639 (the Chinese forecast model data), on 28th Jan.2017 with 489 samples. The upper plot reproduces Figure 1 and is the result of the original GNOS GPS data, and the lower plot isafter implementing the new L2 extrapolation approach.

Atmos. Meas. Tech. Discuss., https://doi.org/10.5194/amt-2018-271
Manuscript under review for journal Atmos. Meas. Tech.
Discussion started: 14 November 2018

Atmospheric Measurement Techniques Discussions

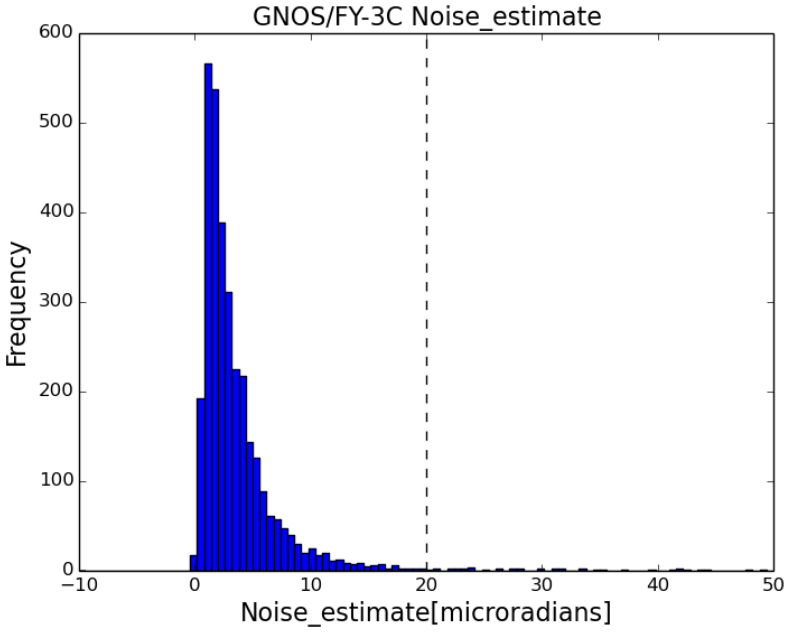

Figure 10. The histogram of the *noise_estimate* parameter using seven days of data from 16th Feb. to 22nd Feb 2017

Atmos. Meas. Tech. Discuss., https://doi.org/10.5194/amt-2018-271
Manuscript under review for journal Atmos. Meas. Tech.
Discussion started: 14 November 2018

Atmospheric Measurement Techniques Discussions

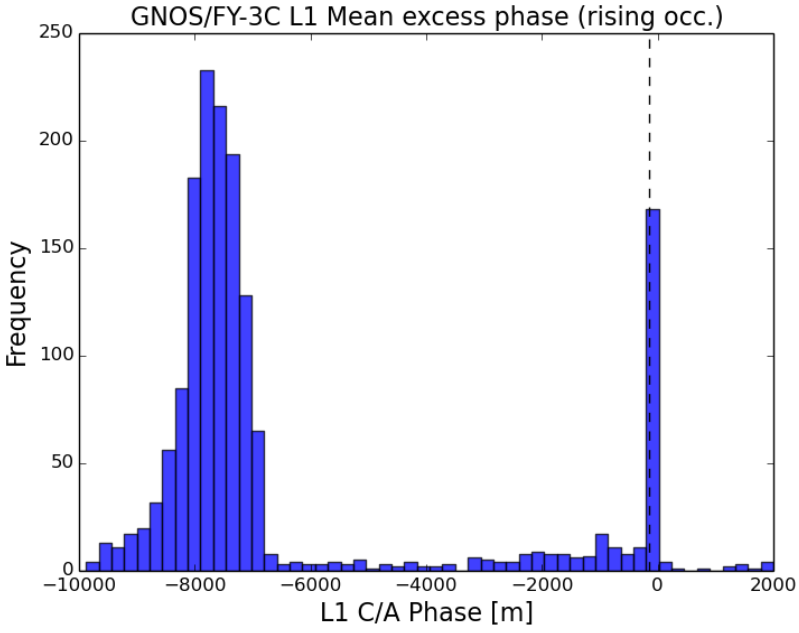

Figure 11. The histograms of L1 mean excess phase for the rising occultation at the height of 60 – 80 km SLTA using seven days of data from 16th Feb. to 22nd Feb.2017.

Atmos. Meas. Tech. Discuss., https://doi.org/10.5194/amt-2018-271
Manuscript under review for journal Atmos. Meas. Tech.
Discussion started: 14 November 2018

Atmospheric Measurement Techniques Discussions

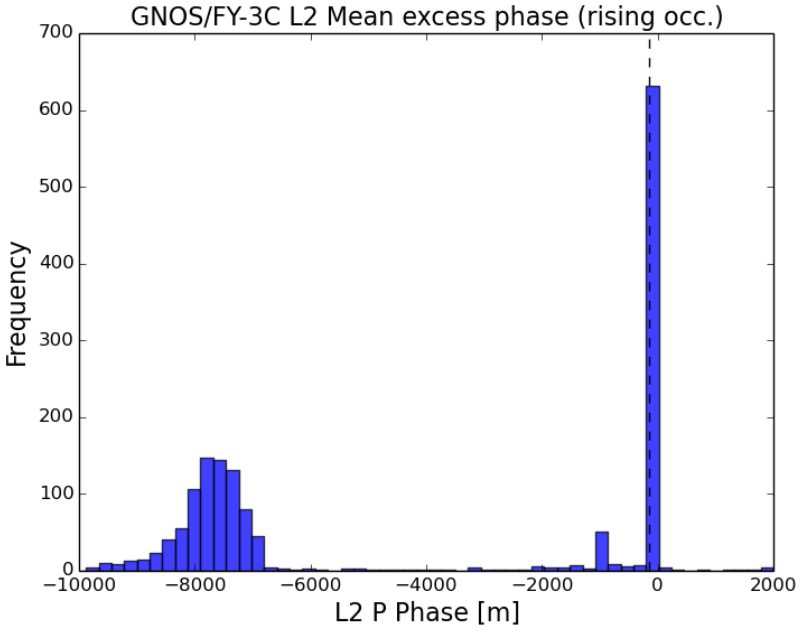

Figure 12. The histograms of L2 mean excess phase for the rising occultation at the height of 60 – 80 km SLTA using seven days of data from 16th Feb. to 22nd Feb.2017.

Atmos. Meas. Tech. Discuss., https://doi.org/10.5194/amt-2018-271
Manuscript under review for journal Atmos. Meas. Tech.
Discussion started: 14 November 2018

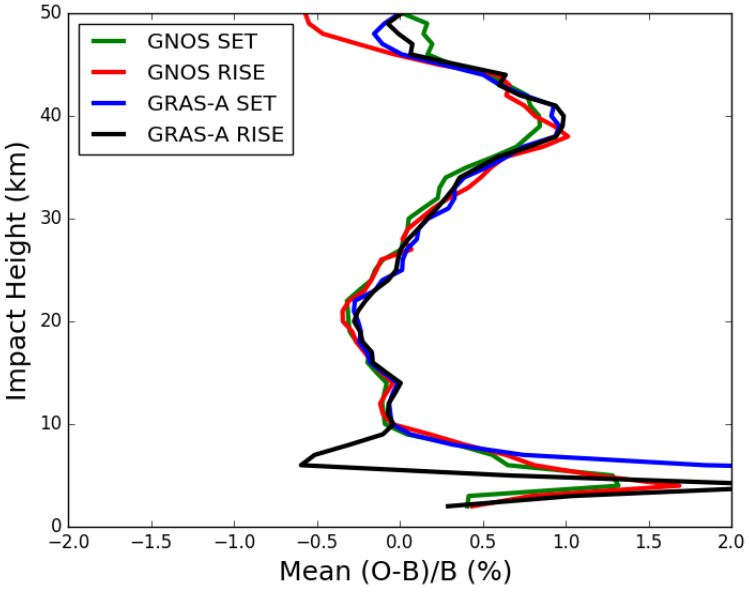

Figure 13. Global bending angle departure results, as a function of impact height, for the mean bias. The green, red, blue and black lines are representative of setting occultation for GNOS, rising occultation for GNOS, setting occultation for GRAS and rising occultation for GRAS.

Atmos. Meas. Tech. Discuss., https://doi.org/10.5194/amt-2018-271
Manuscript under review for journal Atmos. Meas. Tech.
Discussion started: 14 November 2018

Atmospheric Measurement Techniques Discussions

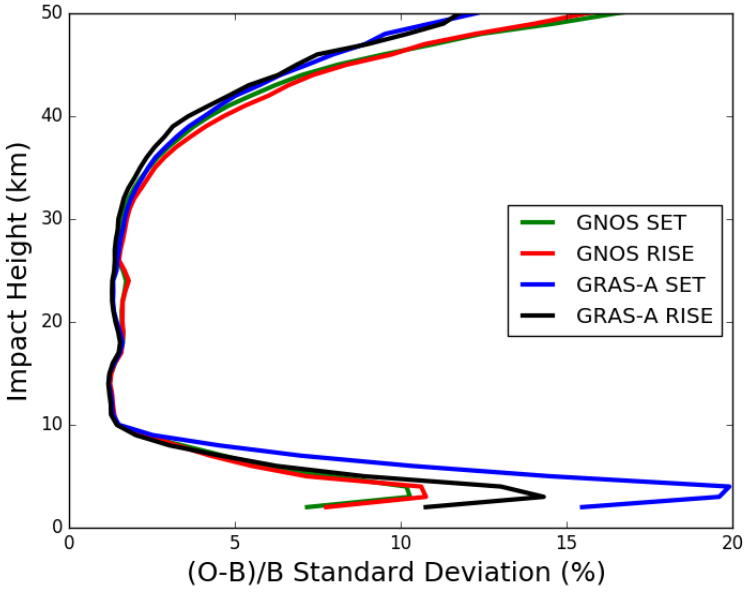

Figure 14. Global bending angle departure results, as a function of impact height, for the standard deviation. The green, red, blue and black lines are representative of setting occultation for GNOS, rising occultation for GNOS, setting occultation for GRAS and rising occultation for GRAS.